Journal of Renewable Materials

Tech Science Press

DOI: 10.32604/jrm.2021.015693

ARTICLE

Improved Geotechnical Behavior of an Expansive Soil Amended with Cationic Polyacrylamide

Shengquan Zhou[1], Minjie Shi[1,*], Wei Chen[1], Yongfei Zhang[1], Weijian Wang[1], Haojin Zhang[1] and Dongwei Li[2]

[1]School of Civil Engineering and Architecture, Anhui University of Science and Technology, Huainan, 232001, China

[2]School of Civil and Architectural Engineering, East China University of Technology, Nanchang, 330013, China

[*]Corresponding Author: Minjie Shi. Email: ytzssmj@163.com

Received: 06 January 2021 Accepted: 01 April 2021

ABSTRACT

The characteristics of soil treated with cationic polyacrylamide (CPAM) mass content of 0%, 0.2%, 0.4%, 0.6%, 0.8%, and 1% were investigated through a series of laboratory tests to explore the practical engineering effect of an expansive soil amended with environmental protection material CPAM. The results indicate that with the increasing CPAM content, the liquid limit and plasticity index of soil decrease, the plastic limit increases, and the free swelling ratio and loaded swelling ratio decrease. Besides, the improved soil has less disintegrating property and better water stability. The shear strength increases as the content increases, and the optimal content is 0.6%. Meanwhile, the cohesion of the soil first increases and then decreases, and the internal friction angle increases. Additionally, the unconfined compressive strength first increases and then decreases. The improved soil presents the characteristics of brittle failure and reaches the peak value (410.1 kPa) at the content of 0.8% after curing for 14 days. Scanning electron microscope (SEM) exhibits that the number of curved and wrinkled sections of the expansive soil is reduced after CPAM improvement. Simultaneously, the arrangement of the superimposed polymer changes from face-face to side-angle or side-face-angle, and the reticular structure formed improves the strength and spatial stability of the soil. Therefore, adding appropriate cationic polyacrylamide could improve expansive soil in engineering.

KEYWORDS

Expansive soil; cationic polyacrylamide; chemical modification; laboratory tests; microstructure

1 Introduction

Expansive soil is a catastrophic soil whose mucilaginous composition is mainly composed of the hydrophilic mineral montmorillonite and illite [1–4]. Expansive soil has the recurrent and potential deformation characteristic of swelling with water absorption and shrinking with water loss [5–8]. In the construction of roads, railways, and underground buildings, the special characteristics of expansive soil often cause more problems in the construction and maintenance of the project [9–16]. Therefore, expansive soil must be improved and treated first to ensure the smooth construction and safety of the project.

Chemical treatment of expansive soil mainly uses the addition of stabilizers [17,18]. Traditional stabilizers such as lime, fly ash, and cement can effectively reduce the swelling ratio of expansive soil

and increase the strength of expansive soil [19–21]. Studies have revealed that the effect of improving expansive soil can be improved by mixing them [22–25]. The microstructure and mineral composition of expansive soil before and after the improvement has been observed by scanning electron microscope (SEM) and X-ray diffraction (XRD) test method. It was demonstrated that these materials all have pozzolanic properties of reducing shrink-swell behavior by chemical reactions between the clay minerals and the calcium oxide molecules at the surface level [26,27]. However, these traditional inorganic ameliorants have problems such as groundwater pollution, great impact on the environment, high dosage, and influence on project progress and cost.

At present, the use of non-traditional stabilizers is becoming more and more popular. Taher et al. [28] compared and evaluated the effectiveness of traditional chemical stabilizers and commercially available polymers in reducing the swelling potential of expansive clays. Tiwari et al. [29,30] discovered that using polypropylene fiber combined with silica fume can effectively improve the shrinkage behavior of expansive soil and increase the CBR value of expansive soil roadbed. Gautam et al. [31] chose a liquid ionic stabilizer composed of sulfuric acid, phosphoric acid, and citric acid, revealing that the swelling rate was effectively reduced in the treated soil compacted with the optimal water content. Besides, salt [32–35] and enzymes [36] can weaken swelling by improving the ionic composition of the soil and reducing the concentration gradient between absorption and free pore water. Natural and synthetic polymers can reduce soil shrinkage and swelling by forming nanocomposite structures [37–40].

Polyacrylamide (PAM) has been used in the improvement of expansive soil [41]. Cationic polyacrylamide (CPAM) is an organic polymer compound [42,43]. This material has good stability and long shelf life. Adding its aqueous solution to the expansive soil in a reasonable proportion has the effect of chemically solidifying the expansive soil and changing the soil structure [44,45]. Considering the influence of organic materials on geotechnical properties [46], the production of CPAM generates little environmental pollution. CPAM is an environmentally friendly material. It is soluble in water, and its aqueous solution is neutral, pollution-free [47]. In this experiment, cationic polyacrylamide (CPAM) is used to improve the expansive soil, and indoor tests are conducted to determine the optimal content, so as to provide scientific suggestions for engineering construction while reducing pollution.

2 Materials

2.1 Expansive Soil

The expansive soil used in the experiment was taken from a construction site in Shannan New District, Huainan City, Anhui Province, China. The soil sample was brown and greyish-yellow. The raw materials for the test are exhibited in Fig. 1. According to the Chinese Standard for Geotechnical Testing Method (GB/T 50123–2019), the physical parameters of test soil were determined by a series of laboratory tests, as presented in Tab. 1. The particle grading curve obtained by the sieve analysis and the particle composition of test soil is provided in Fig. 2 and Tab. 2. As illustrated in Fig. 3, the X-ray diffraction (XRD) result demonstrated that the test soil was primarily composed of quantz and a small amount of albite, illite, and montmorillonite. The main chemical properties of test soil measured by X-ray fluorescence spectroscopy (XRF) are listed in Tab. 3.

2.2 Additives

Polyacrylamide is divided into four types, namely anionic, cationic, non-ionic, and zwitterionic. In this study, cationic polyacrylamide (CPAM), which is a copolymer of acrylamide and cationic monomers, was used as the modifier. The cationic organic matter is connected with multiple N atoms and has a strong positive charge. Due to its polymer effect, it can have sufficient ion exchange adsorption reaction with montmorillonite and illite with a large cation exchange capacity [48,49]. The CPAM used in this research is from Zhengzhou Senhai Water Treatment Co., Ltd., Zhengzhou, China. The main chemical parameters of the additive are listed in Tab. 4.

(a) (b) (c)

Figure 1: Test raw materials. (a) Undisturbed soil sample; (b) Grated soil sample; (c) CPAM sample

Table 1: Physical parameters of Huainan expansive soil

Density (g/cm^3)	Liquid limit (%)	Plastic limit (%)	Plasticity index	Maximum dry density (g/cm^3)	Optimum moisture content (%)	Free swelling ratio (%)
1.98	44.8	23.1	21.7	1.63	22.1	53.8

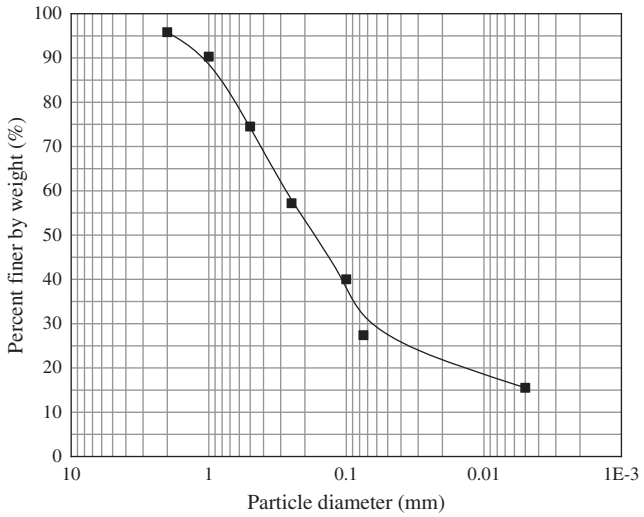

Figure 2: Particle grading curve of expansive soil

Table 2: Particle gradation

Parameter	Particle size						
	$2.0 < d$	$1.0 < d \leq 2.0$	$0.5 < d \leq 1.0$	$0.25 < d \leq 0.5$	$0.075 < d \leq 0.25$	$0.005 < d \leq 0.075$	$d \leq 0.005$
Content (%)	4.2	5.5	15.8	17.3	29.7	11.9	15.6

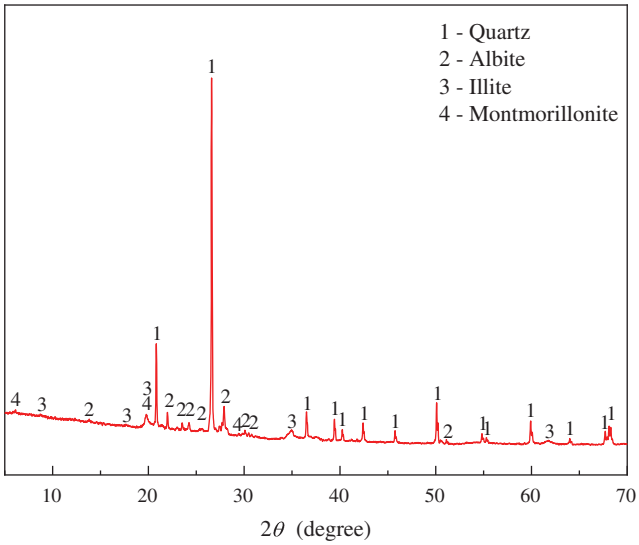

Figure 3: X-ray diffraction of expansive soil

Table 3: Chemical properties of expansive soil

Chemical composition	Content (%)
SiO_2	60.1927
Al_2O_3	16.0402
CO_2	8.3374
Fe_2O_3	6.8768
K_2O	2.9221
CaO	1.4851
TiO_2	0.9991
MgO	0.9875
SO_3	0.5842
P_2O_5	0.5382
Na_2O	0.4296
MnO	0.1481
Cl	0.1109

Table 4: Chemical parameters of CPAM

Appearance	Molecular weight (10 K)	Ion concentration (%)	Solid content (%)	PH	Chemical composition	Structural formula
White powder, granules	800	40	95	7	Acrylamide and cationic monomers	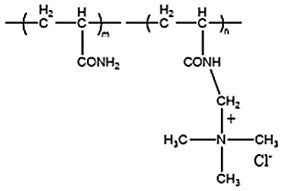

3 Experimental Programs

The physical and mechanical properties were tested in accordance with the Chinese Standard for Geotechnical Testing Method (GB/T 50123-2019), and the content of CPAM was the ratio of the mass of CPAM to the mass of dry soil. The test steps are described as follows:

1. The soil was placed in an oven at 105 degrees Celsius for more than eight hours until it was dried completely. Then, the dried expansive soil was ground and passed through a 0.5 mm sieve. The optimal moisture content was used to weigh the test water. CPAM was added according to the mass percentages of 0.2%, 0.4%, 0.6%, 0.8%, and 1%. Then, it was stirred evenly until dissolved in water. The liquid-plastic limit and free swelling ratio index were determined when CPAM was thoroughly mixed with the test soil.
2. The dried soil was passed through a 2 mm sieve, and the modifier was weighed according to the above ratio and dissolved in water to mix the soil sample. Afterwards, it was put in a sealed bag and cured for 24 h. According to the light compaction standard, cutting ring remolded samples with a diameter of 61.8 mm and a height of 20 mm were prepared. The improved soil was made into a cutting ring sample and placed in a uniaxial consolidation instrument, and a 25 kPa load was applied. After the compression and deformation of the soil sample were stable, water was injected into the water box, and the loaded swelling ratio test was performed. A water stability test was conducted to observe the collapse of the soil sample without confinement. Due to the limited length of the article, only the disintegration diagram of plain soil and 0.6% CPAM improved soil in water were provided. During the direct shear test, the hand wheel rotation and dynamometer readings were recorded. The handwheel speed was 4 r/min, and the normal vertical pressure applied was 50 kPa, 100 kPa, 150 kPa, and 200 kPa.
3. The improved soil was packed into a cylindrical mold with a diameter of 50 mm and a height of 100 mm. All the samples were compacted at the optimum moisture content of 22.1% and dry density of 1.98 g/cm^3. The compaction coefficient of 0.9 was chosen for the production of soil sample [50]. By the layered compaction method, each layer was shaved and compacted into five layers. Three parallel samples were made for each proportion. The samples were wrapped with plastic wrap and put into a sealed bag, enabling the moisture content to be maintained at the curing period of 7 days and 14 days. Besides, the UTM4204 universal testing machine was used in the test. It is controlled by strain during operation and can automatically record the stress-strain curve, with the loading rate of 2 mm/min.
4. The plain soil and improved soil were made into small pieces and dried. Before the SEM test, the soil sample was polished and then plated with gold for 180 s to enhance its conductivity. The acceleration voltage of SEM analysis was set to 20 kV. Flex1000 scanning electron microscope manufactured by Japan Co., Ltd., was used to observe the microstructure of CPAM solid particle, plain soil, and 0.6% CPAM improved soil.

4 Test Results and Analysis

4.1 Liquid-Plastic Limit Test

As indicated in Fig. 4, the boundary moisture content index of the expansive soil significantly improves after the addition of CPAM. With the increasing content of CPAM, the liquid limit and the plasticity index of the improved expansive soil gradually decrease, and the plastic limit gradually increases. With the addition of 1% CPAM as an example, the liquid limit of the improved soil decreases by 6.4%, the plasticity index decreases by 21.6%, and the plasticity increases by 7.8%. This is because the clay minerals (montmorillonite and illite) in the expansive soil have considerable negative charges on the surface. This can be closely related to the added cationic additives, which reduced the thickness of the adsorbed water

film on the surface of the expansive soil particles. Then, the ξ potential [51] (the potential difference between the sliding surface and the solution body, which reflects the charge of the colloidal particles) decreases. The pore space of the soil mass between each particle size shrinks. The soil particles further approach each other and become dense. The internal bound water of the expansive soil decreases. As a result, the liquid limit and plasticity index decrease, and the plastic limit increases.

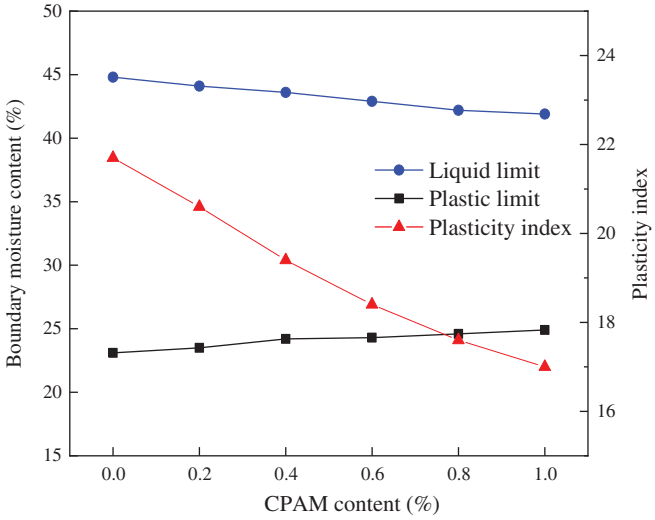

Figure 4: Change of liquid-plastic limit

4.2 Free Swelling Ratio Test

Fig. 5 illustrates that when 0.2% CPAM is added, the free swelling ratio of the improved soil drops to 39.1%, making it no longer belongs to expansive soil, according to the Technical Code for Building in Expansive Soil Regions (GB 50112-2013). Similar to traditional modifiers [52], the free swelling ratio decreases with the increase of CPAM content at the beginning. However, the free swelling ratio begins to increase again when the content exceeds 0.6%. This is because when the content is low, the adsorption capacity of the active part of CPAM to clay under the action of electrostatic and hydrogen bonding increases with the increasing content. However, when exceeding a content, the adsorption capacity will reach saturation. It was discovered during the experiment that flocs had formed in the water when 0.6% CPAM was stirred and dissolved in water. This floc weakens the adsorption and bridging effect between CPAM and expansive soil. Consequently, the expansibility of the improved soil increases again. The change curves of the two curing periods in Fig. 5 are close to coinciding since CPAM improvements are conducted in solution without hydration reaction.

4.3 Loaded Swelling Ratio Test

It can be observed from Fig. 6a that the soil sample shrinks and deforms in the first 140 min under the load of 25 kPa. After the deformation is stable, the soil sample expands rapidly in the next 80 min under the water injection condition. The growth rate of the loaded expansion gradually decreases until it stabilizes. As illustrated in Fig. 6b, the loaded swelling ratio decreases with the increasing CPAM content. Specifically, considerable amino groups on the CPAM molecular chain can form hydrogen bonds with the oxygen and hydrogen-oxygen layers on the mineral crystal surface. Consequently, a thin film is formed on the surface of the expansive soil particles. This strong electrostatic effect weakens the negative electric repulsion between the layers and prevents the infiltration of external water from increasing the interlayer spacing to form expansion, reducing the loaded swelling ratio. It is noteworthy that the loaded swelling ratio

increases again when the content of CPAM exceeds 0.8%. Because when the content of CPAM exceeds a value, its adsorption on the surface of the clay reaches saturation, and excessive polyacrylamide causes the swelling of the soil to increase again.

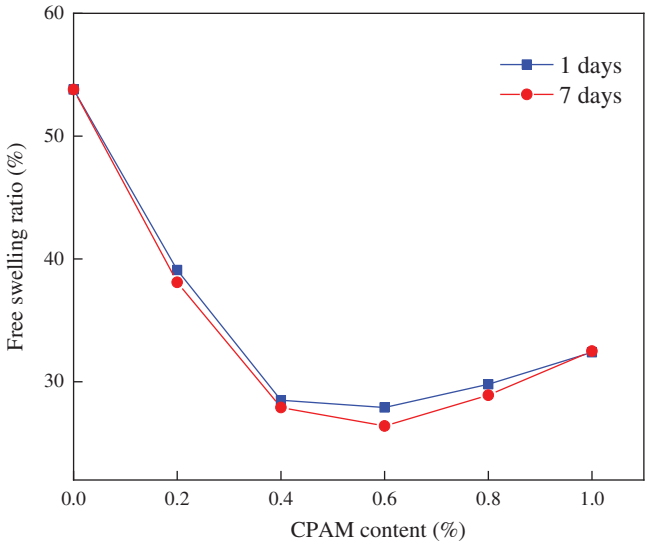

Figure 5: Change of free swelling ratio

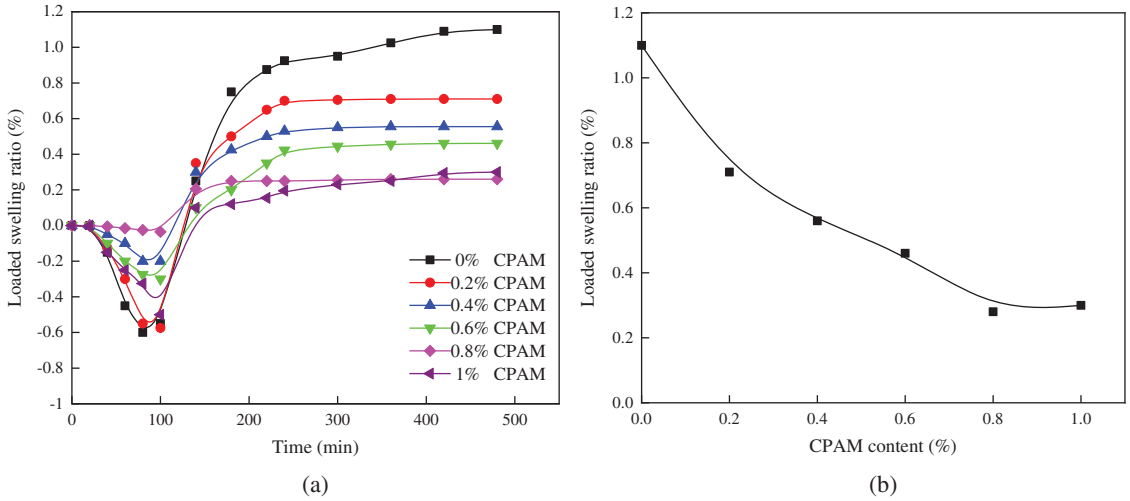

Figure 6: Effect of CPAM on the loaded swelling ratio. (a) Aging diagram of loaded swelling ratio; (b) Change of loaded swelling ratio

4.4 Water Stability Test

As presented in Fig. 7, the plain soil began to fall off in blocks at 0.5 h, floating bubbles increased, the upper surface edge gradually lifted up, and cracks appeared. After 1 h, the collapse intensified, the upper edge became loose and fell off, and the surface was covered with cracks. Then, the upper surface cracks moved towards the middle basically stabilized after 4 h and disintegrated after 6 h. The 0.6% CPAM improved soil began to loosen at the edge at 0.5 h, and cracks appeared on the upper surface edge for 1–4 h and gradually extended to the middle. The edge loosening increased while no soil debris slipped. After 6 h, the crack width

increased. The improved soil sample is intact as a whole because CPAM reacts with montmorillonite and illite to form a covering film that connected and wrapped the soil particles. The hydrophilicity of the improved soil is fundamentally changed, contributing to forming a reticular structure and making a closer connection between the soil particles. This improved feature enhances the water stability of the soil, beneficial to the construction of expansive soil embankments and slopes in rainy areas.

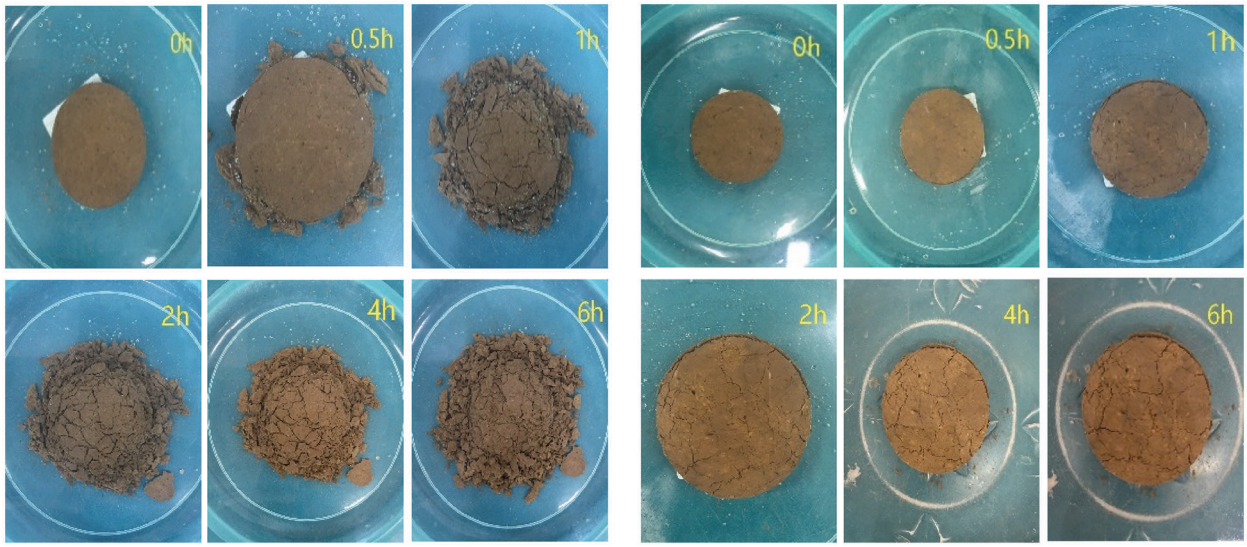

Figure 7: Disintegration diagrams in water. (a) Disintegration diagrams of plain soil; (b) Disintegration diagrams of 0.6% CPAM improved soil

4.5 Direct Shear Test

Fig. 8 presents the stress-displacement curves of different contents. The shear strength under different overburden pressures is listed in Tab. 5. The shear strength fitting curves and the test data summary are exhibited in Fig. 9 and Tab. 6.

Fig. 8 indicates that the shear strength of expansive soil is related to the normal vertical pressure. The peak strength of plain soil and improved soil increases with the increasing overburden pressure, and the residual strength still meets this law. This is because the upper soil and the lower soil are squeezed to produce relative displacement when the soil subjected to horizontal thrust, resulting in a large "bite" force needing to be overcome. The greater the overburden pressure, the greater the bite force needing to be overcome, and the greater the shear strength. Particularly, the stress-displacement curves first increase and then decrease to be stable regardless of plain soil or improved soil. The soil particles can bypass another part of the soil particles when the shear strength of the soil itself is greater than the bite force. At this time, the integral structure of the soil becomes loose. A significant displacement occurs in the upper and lower parts of the soil. Meanwhile, the shear resistance is weakened and the softening characteristics are shown. The data in Tab. 5 demonstrate that the shear strength of the soil increases as the CPAM content increases at the same overburden pressure. However, the increase in shear strength begins to slow down when the content exceeds 0.6%. Under the overburden pressure of 150 kPa, the shear strength of 0.8% CPAM is even lower than 0.6% CPAM, suggesting that there is an optimal content for CPAM.

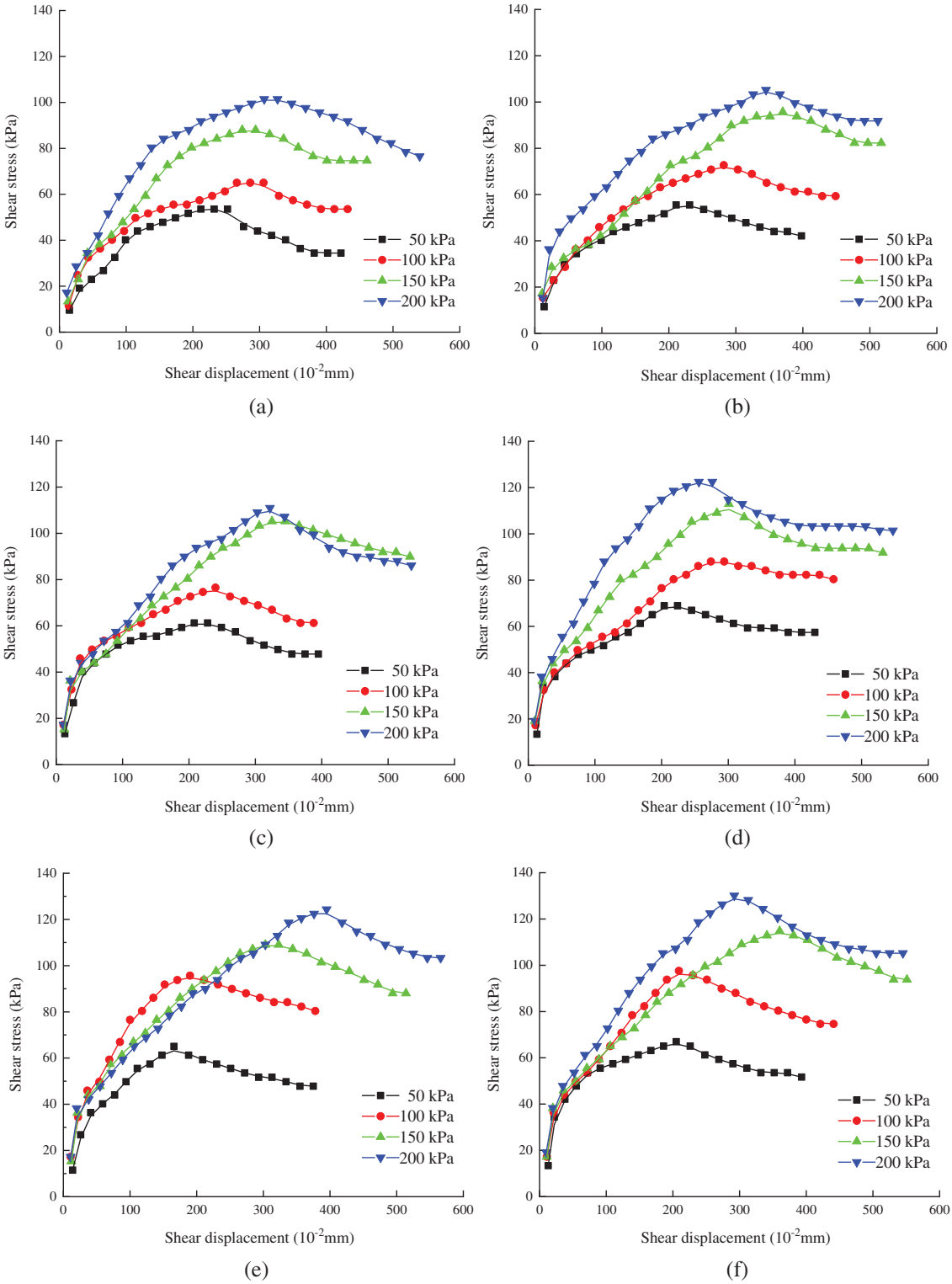

Figure 8: The relationship curves of shear stress-displacement under different CPAM contents. (a) 0% CPAM content; (b) 0.2% CPAM content; (c) 0.4% CPAM content; (d) 0.6% CPAM content; (e) 0.8% CPAM content; (f) 1% CPAM content

Table 5: Shear strength under different overburden pressures

Overburden pressure (kPa)	Shear strength under different CPAM content (kPa)					
	0%	0.2%	0.4%	0.6%	0.8%	1%
50	53.57	55.49	61.23	68.88	65.05	66.97
100	65.05	72.71	76.53	88.01	95.67	97.58
150	88.01	95.67	105.28	112.89	109.06	114.80
200	101.41	105.23	110.97	122.45	124.37	130.11

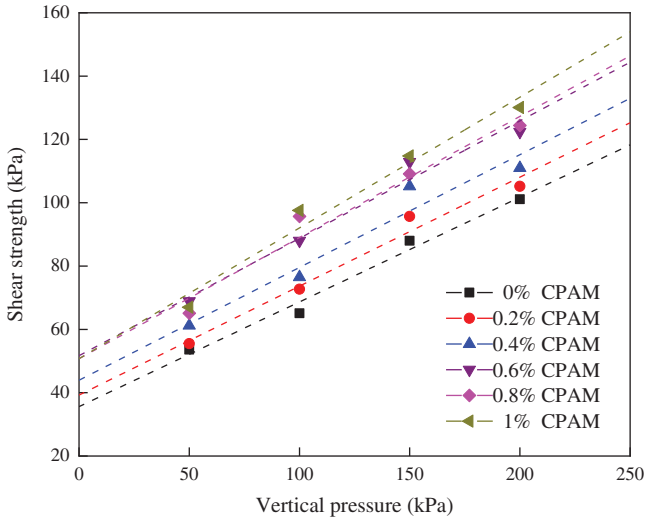

Figure 9: Fitting curves for shear strength

Table 6: Summary of direct shear test data

Soil type	Swelling potential	Linear fit relationship equation	Shear strength index			Compared to plain soil		
			c/kPa	$\varphi/^{\circ}$	Δc	$\frac{\Delta c}{c}$	$\Delta\varphi$	$\frac{\Delta\varphi}{\varphi}$
Plain soil	Weak	y = 0.33x + 35.60	35.60	18.26	0.00	0.00	0.00	0.00
0.2% CPAM	None	y = 0.34x + 39.25	39.25	18.77	3.65	0.10	0.51	0.03
0.4% CPAM	None	y = 0.35x + 43.95	43.95	19.39	8.35	0.23	1.13	0.06
0.6% CPAM	None	y = 0.37x + 51.70	51.70	20.30	16.10	0.45	2.04	0.11
0.8% CPAM	None	y = 0.38x + 50.75	50.75	20.81	15.15	0.43	2.55	0.14
1% CPAM	None	y = 0.41x + 49.98	49.98	22.29	14.38	0.40	4.03	0.22

As indicated in the fitted curves in Fig. 9, the shear strength and vertical pressure of the improved soil were linearly related after the addition of CPAM. The data in Tab. 6 reveal that at the content of 0%–0.6%, the cohesive force and internal friction angle of the improved soil sample increase with the increase of CPAM

content. After the addition of CPAM, the cementation effect makes the connection between soil particles closer and tighter. Consequently, the particle connection strength and the shear strength are enhanced. Regarding the improvement effect, with the application of 200 kPa vertical pressure as an example, the increase of cohesion of CPAM improved soil with the content of 0.2%, 0.4%, 0.6%, and 0.8% is 10%, 23%, 45%, and 43%, and the increase of internal friction angle is 3%, 6%, 11%, and 14%, respectively. However, the internal friction angle continues to increase while the cohesive force tends to decrease when the content exceeds 0.6%. From one perspective, the shear strength of the soil is determined by both the internal friction angle and the cohesion. From another perspective, CPAM cannot greatly increase the effect of improving the strength of expansive soil when the content is too high. Thus, it is confirmed that there is an optimal content of CPAM. According to the Cullen formula $\tau = c + \sigma \tan \varphi$ in Soil Mechanics and from an economic point of view, the content of 0.6% is a reasonable value.

4.6 Unconfined Compressive Strength Test

An unconfined compressive strength (UCS) test was conducted to further investigate the improvement effect of CPAM content on the strength of expansive soil. The damage patterns of the specimens are presented in Fig. 10.

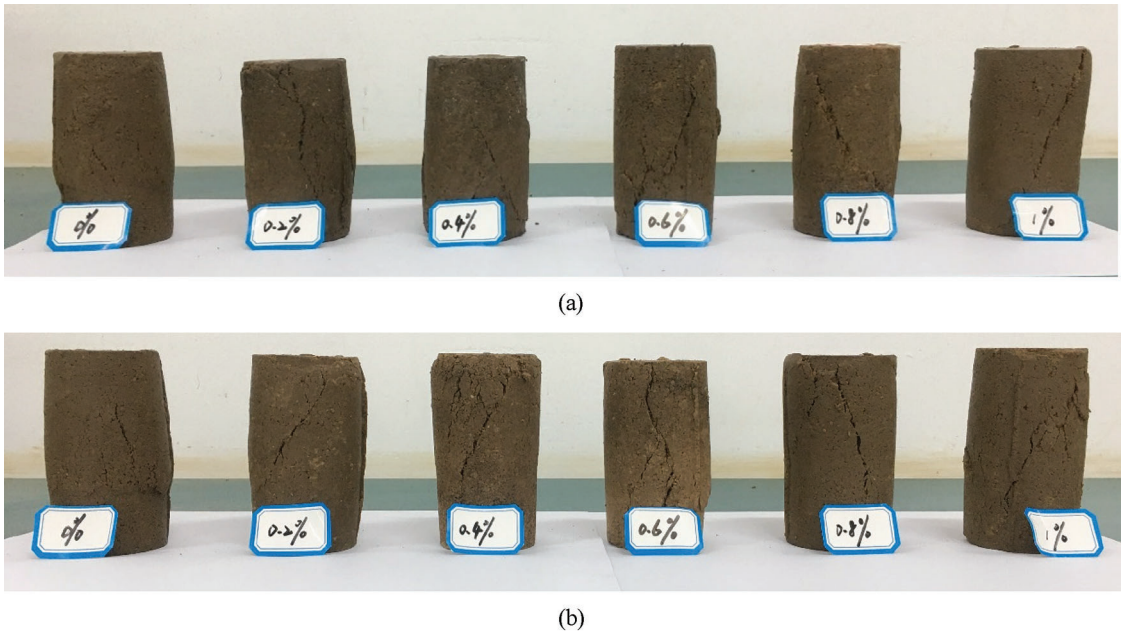

Figure 10: Damage patterns under different curing periods. (a) Curing for 7 days; (b) Curing for 14 days

Stress-strain curves of different curing periods are shown in Fig. 11, and the growth law of the unconfined compressive strength of improved soil is shown in Fig. 12.

The stress-strain relationship curves of the improved soil with the corresponding content of different periods are exhibited in Figs. 11a and 11b. At the curing period of 7 days, the stress-strain curves of plain soil, 0.2% CPAM and 0.4% CPAM present a strain hardening type, with significant plastic characteristics and a yield platform. At the curing period of 14 days, the stress-strain curves of the improved soil are different (only the elastic stage and the damage stage), the overall trend of curves starts to show a strain-softening type after 0.6% content, and the strength of the improved soil reaches the peak and then immediately decreases, presenting the characteristics of brittle damage.

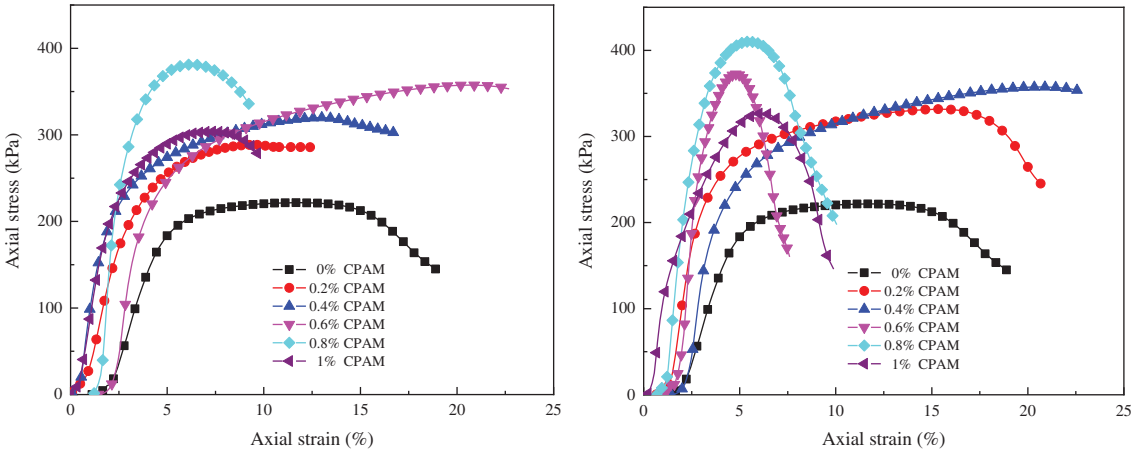

Figure 11: Typical stress-strain curves of improved soil under different curing periods. (a) Curing for 7 days; (b) Curing for 14 days

Fig. 12a shows the unconfined compressive strength of the improved soil at different curing periods with different CPAM content. Fig. 12b exhibits the growth law of the unconfined compressive strength of the improved soil at 7 days and 14 days in curing periods. Under different contents, the increasing law of strength after curing for 7 days presents a wavy change pattern. The growth rate of strength increases from 30.1% to 72.1% and then drops to 37.1%. With the increasing content, the unconfined compressive strength of the improved soil first increases and then decreases, and 0.8% is the optimal content. The strength-growth rate of the specimens at 14 days curing periods shows the same law as 7 days while growth rates of 14 days relative to 7 days were 14.9%, 11.9%, 5.0%, 7.5%, and 7.7%, respectively, which were not significant. This is because the reaction between CPAM and clay minerals occurs in the form of ion exchange and does not involve hydration, which is different from lime, fly ash, and cement improvement. Thus, the period of curing has little effect on the unconfined compressive strength.

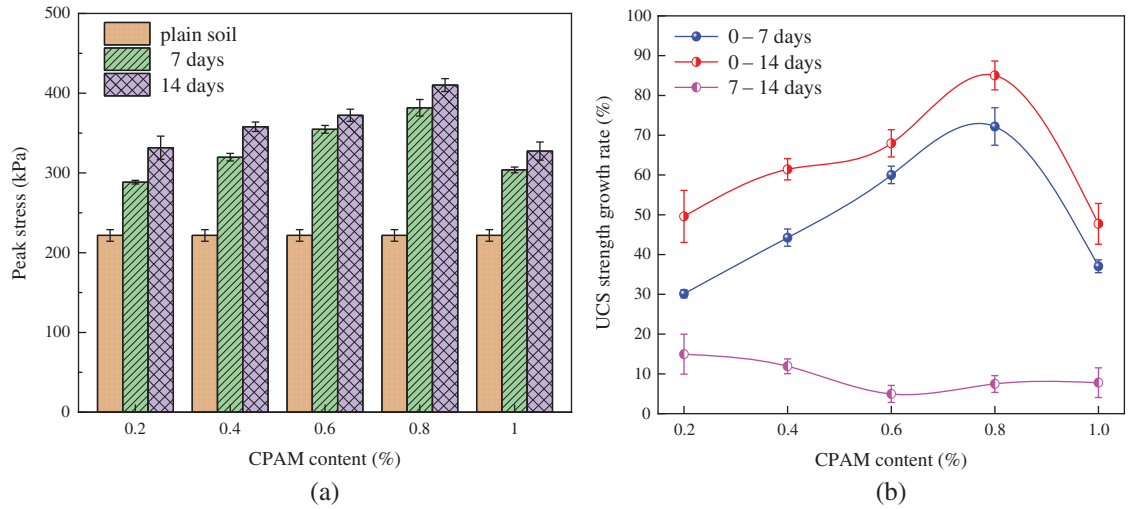

Figure 12: Relationship between the unconfined compressive strength and curing period of the improved soil with different CPAM content. (a) Peak stress diagram; (b) USC strength growth rate at different curing periods

4.7 Micro-Analysis

A scanning electron microscope test was conducted to compare the microstructure changes of expansive soil before and after improvement.

As indicated in Fig. 13, at a magnification of 500, the CPAM solid particles are tightly interconnected with particles and wrapped around each other. When the magnification is 1000, local flocs are presented with high viscosity and mutual adsorption. At 5000 magnification, particles are colloidal. This colloid enables the molecules to present an adsorption and bridging effect. A covering film is formed on its surface when reacting with clay minerals such as montmorillonite and illite. On the one hand, it promotes closer interparticle connections, and on the other hand, it prevents the passage of external water from penetrating the soil, reducing the hydrophilicity of expansive soil.

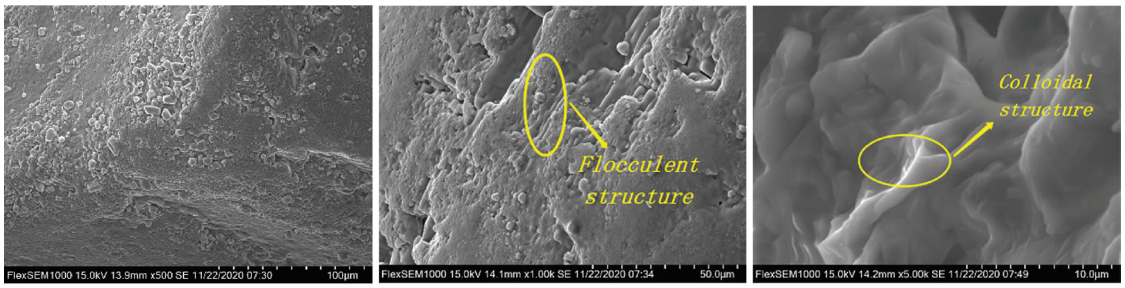

(×500) (×1000) (×5000)

Figure 13: SEM images of CPAM

The scanning electron microscope images of plain soil are illustrated in Fig. 14. After 500 times magnification, the swelling clay consists of laminated intergranular associations and face-to-face superimposed polymer in the form of scales, and this superimposition forms the organizing unit for the swelling and shrinking effect. When the magnification is 1000, the shape of the surface clay is not only flat and straight but also curved and wrinkled, and the edge shape is clear or fuzzy. Under 5000 times magnification, the flaky distribution of particles is more clearly. These particles are curved and wrinkled without edges. These are particles of montmorillonite or mixed layers of montmorillonite and illite, contributing to the main cause of the expansion and shrinkage of expansive soil.

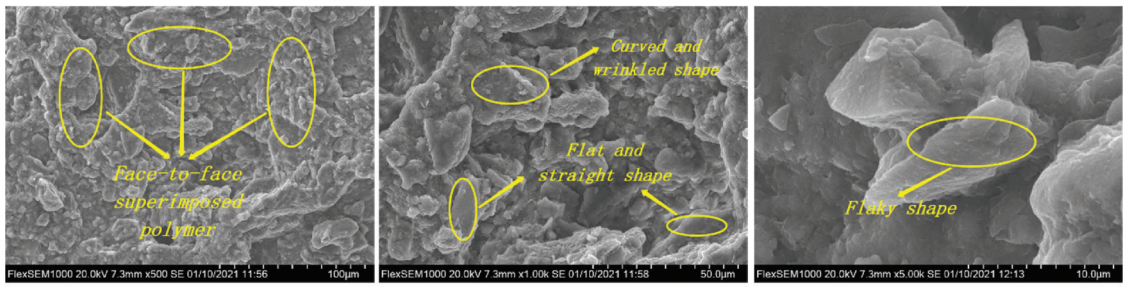

(×500) (×1000) (×5000)

Figure 14: SEM images of plain soil

Fig. 15 provides the SEM images of the 0.6% CPAM improved soil. Under 500 times magnification, the arrangement of superimposed polymer is sparser. Therefore, the swelling pressure of the improved soil becomes smaller after water immersion, reducing the degree of swelling and exhibiting expansion. When

the magnification is 1000, the cementing effect of CPAM changes the connection of superimposed polymer to side-angle or side-face-angle arrangement, which has a certain reticular structure. Under 5000 times magnification, the number of curved lamellar particles (montmorillonite or mixed layers of montmorillonite and illite) is reduced, explaining the decreasing swelling potential of the improved soil. Moreover, the reticular structure forming between the particles could be more visually observed to further improve the stability of the soil and enhance its strength.

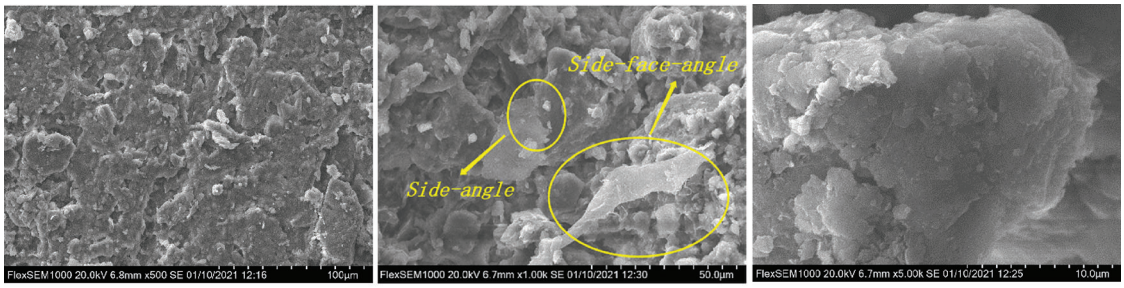

(×500) (×1000) (×5000)

Figure 15: SEM images of 0.6% CPAM improved expansive soil

5 Conclusions

CPAM weakens the negative electric repulsion between layers and prevents the expansion of the interlayer space through the adsorption and electrostatic action generated by the polymer effect, improving the strong hydrophilicity of clay minerals.

With the increasing CPAM content, the plastic limit of expansive soil increases, the liquid limit and plasticity index decrease, and the free swelling ratio and the loaded swelling ratio both first decrease and then increase.

The disintegration in the water of the CPAM improved soil cutting ring remolded sample is stable, and the water stability is significantly better than that of plain soil, contributing to the construction of expansive soil embankments and slopes in rainy areas.

The shear strength of plain soil and improved soil increase as the overburden pressure increases, and the shear strength of improved soil increases with the increasing CPAM content. Meanwhile, the cohesion first increases and then decreases, and the internal friction angle increases. The optimum content is 0.6%.

With the incorporation of CPAM, the stress-strain curve of expansive soil changes from stress-hardening type to stress-softening type, indicating the characteristic of brittle damage. The unconfined compressive strength first increases and then decreases. The content of the peak value (410.1 kPa) is 0.8%.

Scanning electron microscopic analysis reveals that plain soil is mainly composed of face-to-face superimposed polymer with curved and wrinkled soil particles, and the CPAM changes the connection of superimposed polymer to side-angle or side-face-angle arrangement, forming a reticular structure. This structure can improve the bond strength between expansive soil particles and make the soil have higher strength and deformation rate, demonstrated as the increase in shear strength and uniaxial compressive strength.

Expansive soil improved with Cationic polyacrylamide has the advantages of saving time, less construction amount, and environmental protection. The evaluation of the improved effect between CPAM and traditional stabilizers still needs to be further studied and discussed in subsequent experiments.

Acknowledgement: The authors sincerely thank the School of Civil Engineering and Architecture, State Key Laboratory of Mining Response and Disaster Prevention and Control in Deep Coal Mine in Anhui University of Science and Technoloy for providing the experiment conditions.

Funding Statement: This research was funded by the National Natural Science Foundation of China (41977236, 41672278, 41271071), the Science and Technology Planning Project of Housing and Urban-Rural Development of Anhui Province (2019-YF023), the Major Universities Natural Science Research Project in Anhui Province (KJ2016SD19), and the Natural Science Foundation of Jiangxi Province (2019ACBL20002).

Conflicts of Interest: The authors declare that they have no conflicts of interest to report regarding the present study.

References

1. Wang, B. T., Zhang, F. H. (2008). *Improving technology and engineering application of expansive soil*. China: Science Press.
2. Li, S. L. (1992). *Engineering geology of swelling soils in china*. China: Jiangsu Science and Technology Press.
3. Mohanty, S. K., Pradhan, P. K., Mohanty, C. R. (2017). Stabilization of expansive soil using industrial wastes. *Geomechanics and Engineering, 12(1),* 111–125. DOI 10.12989/gae.2017.12.1.111.
4. Samuel, R., Puppala, A. J., Radovic, M. (2020). Sustainability benefits assessment of metakaolin-based geopolymer treatment of high plasticity clay. *Sustainability, 12,* 10495. DOI 10.3390/su122410495.
5. Zhao, S. Y., Shi, Z. M., Peng, M., Bao, Y. N. (2020). Stability analysis of expansive soil slope considering seepage softening and moistening expansion deformation. *Water, 12,* 1678. DOI 10.3390/w12061678.
6. Tiwari, N., Satyam, N. (2019). Experimental study on the influence of polypropylene fiber on the swelling pressure expansion attributes of silica fume stabilized clayey soil. *Geosciences, 9,* 377. DOI 10.3390/geosciences9090377.
7. Khan, S., Ivoke, J., Nobahar, M. (2019). Coupled effect of Wet-dry cycles and rainfall on highway slope made of yazoo clay. *Geosciences, 9,* 341. DOI 10.3390/geosciences9080341.
8. Dai, Z., Guo, J., Luo, H., Li, J., Chen, S. (2020). Strength characteristics and slope stability analysis of expansive soil with filled fissures. *Applied Sciences, 10(4616),* 4616. DOI 10.3390/app10134616.
9. Liu, T. H. (1997). *Expansive soil problems in engineering construction*. China: China Construction Industry Press.
10. Rosales, J., Agrela, F., Marcobal, J. R., Diaz-Lopez, J. L., Cuenca-Moyano, G. M. et al. (2020). Use of nanomaterials in the stabilization of expansive soils into a road real-scale application. *Materials, 13(14),* E3058. DOI 10.3390/ma13143058.
11. Ahmed, A., Hossain, M. S., Pandey, P., Sapkota, A., Thian, B. (2019). Deformation modeling of flexible pavement in expansive subgrade in texas. *Geosciences, 9,* 446. DOI 10.3390/geosciences9100446.
12. Cai, Y. J., Yang, Y. H., Zhang, L. P., Li, L. (2016). *Engineering geology of expansive soils for the south-north water diversion central line project*. China: Changjiang Press.
13. Far, H., Flint, D. (2017). Significance of using isolated footing technique for residential construction on expansive soils. *Frontiers of Structural and Civil Engineering, 11(1),* 123–129. DOI 10.1007/s11709-016-0372-8.
14. Mockbee, D. W., Jones, J. R. (2011). Engineer's legal exposure for facilities built on expansive soils. *Journal of Performance of Constructed Facilities, 25(1),* 7–17. DOI 10.1061/(ASCE)CF.1943-5509.0000106.
15. Sorochan, E. A. (2020). *Construction of buildings on expansive soils*. USA: CRC Press.
16. Nelson, E. J., Chao, K. C., Nelson, J. D., Overton, D. D. (2017). Lessons learned from foundation and slab failures on expansive soils. *Journal of Performance of Constructed Facilities, 31(3),* 1–14. DOI 10.1061/(ASCE)CF.1943-5509.0000958.
17. Qiu, X. L., Wang, B. T. (2013). Experimental study on the effect of chemical improvement of swelling soil and its application in slope engineering. *Journal of Water Resources and Construction Engineering, 11(2),* 190–195. DOI 10.3969/j.issn.1672-1144.2013.02.042.

18. Yu, H. Z., Li, S. Q., Yao, J. W. (2006). Analysis of experimental research on chemical improvement of expansive soils. *Geotechnics, 11,* 1941–1944. DOI 10.16285/j.rsm.2006.11.015.
19. Zhuang, X. S., Peng, W. K., Wu, J. B. (2017). Experimental study on the strength of lime modified expansive soil. *Highway Engineering, 42(5),* 1–5. DOI 10.3969/j.issn.1674-0610.2017.05.001.
20. Zha, F. S., Liu, S. Y., Du, Y. J. (2007). Experiment on lime-fly ash improvement of swelling soil. *Journal of Southeast University (Natural Science Edition), 2,* 339–344. DOI 10.3321/j.issn:1001-0505.2007.02.031.
21. Lu, Y., Liu, S. H., Zhang, Y. G., Li, Z., Xu, L. (2020). Freeze-thaw performance of a cement-treated expansive soil. *Cold Regions Science and Technology, 170,* 102926. DOI 10.1016/j.coldregions.2019.102926.
22. Hui, H. Q., Hu, T. K., Wang, X. D. (2006). Mechanism of lime and fly ash improvement of swelling soil properties. *Journal of Chang'an University (Natural Science Edition), 2,* 34–37. DOI 10.19721/j.cnki.1671-8879.2006.02.009.
23. Zhou, S. Q., Zhou, D. W., Zhang, Y. F., Wang, W. J. (2019). Research on the dynamic mechanical properties and energy dissipation of expansive soil stabilized by fly ash and lime. *Advances in Materials Science and Engineering, 2019,* 5809657, DOI 10.1155/2019/5809657.
24. Xiao, J., Wang, B. T., Sun, Y. C., Zhang, F. H., Feng, X. S. (2012). Experiment on composite improvement of swelling soil with cement and lime. *South-North Water Diversion and Water Conservancy Science and Technology, 10(2),* 9–13. DOI 10.3724/SP.J.1201.2012.02009.
25. Khadka, S. D., Jayawickrama, P. W., Senadheera, S., Segvic, B. (2020). Stabilization of highly expansive soils containing sulfate using metakaolin and fly ash based geopolymer modified with lime and gypsum. *Transportation Geotechnics, 23,* 100327. DOI 10.1016/j.trgeo.2020.100327.
26. Ma, X. N., Wang, X. C., Sun, J. L., Wang, H., Fu, L. J. (2016). Microstructure and swelling properties of expansive soil in longnan area. *South-to-North Water Diversion and Water Conservancy Science and Technology, 14(3),* 111–114+149. DOI 10.13476/j.cnki.nsbdqk.2016.03.020.
27. James, J. (2020). Sugarcane press mud modification of expansive soil stabilized at optimum lime content: Strength, mineralogy and microstructural investigation. *Journal of Rock Mechanics and Geotechnical Engineering, 12(2),* 395–402. DOI 10.1016/j.jrmge.2019.10.005.
28. Taher, Z. J., Scalia IV, J., Bareither, C. A. (2020). Comparative assessment of expansive soil stabilization by commercially available polymers. *Transportation Geotechnics, 24,* 100387. DOI 10.1016/j.trgeo.2020.100387.
29. Tiwari, N., Satyam, N., Patva, J. (2020). Engineering characteristics and performance of polypropylene fibre and silica fume treated expansive soil subgrade. *International Journal of Geosynthetics and Ground Engineering, 6(2),* 18. DOI 10.1007/s40891-020-00199-x.
30. Tiwari, N., Satyam, N., Singh, K. (2020). Effect of curing on micro-physical performance of polypropylene fiber reinforced and silica fume stabilized expansive soil under freezing thawing cycles. *Scientific Reports, 10(1),* 7624. DOI 10.1038/s41598-020-64658-1.
31. Gautam, S., Hoyos, L. R., He, S., Prabakar, S., Yu, X. B. (2020). Chemical treatment of a highly expansive clay using a liquid ionic soil stabilizer. *Geotechnical and Geological Engineering, 38(5),* 4981–4993. DOI 10.1007/s10706-020-01342-1.
32. Hattamleh, O. A., Aldeeky, H., Rabab'ah, S., Taamneh, A. (2020). The effect of dead Sea salt solution on the engineering properties of expansive subgrade clayey soil. *Arabian Journal of Geosciences, 13(11),* 405. DOI 10.1007/s12517-020-05364-0.
33. Taiwo, O. D., Joseph, O. A., Kunle, E. O. (2018). Experimental datasets on engineering properties of expansive soil treated with common salt. *Data in Brief, 18(1),* 1277–1281. DOI 10.1016/j.dib.2018.04.038.
34. Zou, W. L., Ye, J. B., Han, Z., Vanapalli, S. K., Tu, H. Y. (2018). Effect of montmorillonite content and sodium chloride solution on the residual swelling pressure of an expansive clay. *Environmental Earth Sciences, 77(19),* 1. DOI 10.1007/s12665-018-7873-9.
35. Xu, Y. F. (2020). Hydraulic mechanism and swelling deformation theory of expansive soils. *Chinese Journal of Geotechnical Engineering, 42(11),* 1979–1987. DOI 10.11779/CJGE202011002.

36. Pooni, J., Giustozzi, F., Robert, D., Setunge, S., O'Donnell, B. (2019). Durability of enzyme stabilized expansive soil in road pavements subjected to moisture degradation (Review). *Transportation Geotechnics, 21,* 100255. DOI 10.1016/j.trgeo.2019.100255.
37. Azzam, W. R. (2014). Behavior of modified clay microstructure using polymer nanocomposites technique. *Alexandria Engineering Journal, 53(1),* 143–150. DOI 10.1016/j.aej.2013.11.010.
38. Soltani, A., Deng, A., Taheri, A., Mirzababaei, M. (2018). Rubber powder-polymer combined stabilization of south Australian expansive soils. *Geosynthetics International, 25(3),* 304–321. DOI 10.1680/jgein.18.00009.
39. Mirzababaei, M., Arulrajah, A., Horpibulsuk, S., Soltani, A., Khayat, N. (2018). Stabilization of soft clay using short fibers and poly vinyl alcohol. *Geotextiles and Geomembranes, 46(5),* 646–655. DOI 10.1016/j.geotexmem.2018.05.001.
40. Tiwari, N., Satyam, N. (2020). An experimental study on the behavior of lime and silica fume treated coir geotextile reinforced expansive soil subgrade. *Engineering Science and Technology, An International Journal, 23(5),* 1214–1222. DOI 10.1016/j.jestch.2019.12.006.
41. Soltani, A., Deng, A., Taheri, A., O'Kelly, B. C. (2019). Engineering reactive clay systems by ground rubber replacement and polyacrylamide treatment. *Polymers, 11(10),* 1675. DOI 10.3390/polym11101675.
42. Yu, X. W., Fu, C. L., Gu, A. Q., Han, Y., Wang, J. M. et al. (2017). Study on synthetic process conditions and flocculation performance of cationic polyacrylamide. *Chemical Research and Application, 29(3),* 319–324. DOI 10.3969/j.issn.1004-1656.2017.03.006.
43. Cao, J. P., Zhang, S., Han, B. L. (2011). Synthesis and characterization of cationic polyacrylamide flocculant. *Journal of Beijing University of Chemical Technology (Natural Science Edition), 4,* 52–57. DOI 10.13543/j.cnki.bhxbzr.2011.04.028.
44. Wang, J., Jiang, J. L., Zhang, J. B. (2014). Comparative experimental study on two modification schemes of expansive soil. *Science and Technology Horizon, 25,* 142–143. DOI 10.19694/j.cnki.issn2095-2457.2014.25.110.
45. Zhang, W. L., Li, Y. H., Dang, J. Q., Wang, F. (2015). Study on improving the accuracy of free swelling ratio test. *Journal of Northwest Agriculture and Forestry University (Natural Science Edition*), *43(9),* 203–209. DOI 10.13207/j.cnki.jnwafu.2015.09.029.
46. Estabragh, A. R., Afsari, E., Javadi, A. A., Babalar, M. (2020). Effect of two organic chemical fluids on the mechanical properties of an expansive clay soil. *Journal of Testing and Evaluation, 48(5),* 3501–3514. DOI 10.1520/jte20170623.
47. Ma, C. P., Zhou, Y. H., Zhang, J., Kang, M. X., Ning, F. et al. (2020). Progress in preparation and application of cationic polyacrylamide. *Chemical New Materials, 48(6),* 226–231. DOI 10.19817/j.cnki.issn1006-3536.2020.06.050.
48. Wang, Y. X, Guo, P. P., Shan, S. B., Qian, Y. L., Lv, W. K. (2015). Experimental research and micromechanism analysis for expansive soil of hefei improved by cation. *Industrial Construction, 45(9),* 104–109+135. DOI 10.13204/j.gyjz201509022.
49. Wang, Y. P., Hu, R. L., Li, Z. Q., Li, C. C. (2008). Field experiment on chemical modified treatment of expansive soil embankment. *Journal of Engineering Geology, 16(1),* 124–129. DOI 10.3969/j.issn.1004-9665.2008.01.022.
50. Gao, X. B., Ruan, B., Tian, X. T., Lv, Y. Y., Li, S. J. et al. (2014). Experiment study on unconfined compressive strength of lime stabilized expansive soil in guizhou province. *Journal of Railway Science and Engineering, 11(6),* 68–71. DOI 10.19713/j.cnki.43-1423/u.2014.06.012.
51. Liu, G. P., Wei, P. H., Zhang, Y. C. (2005). The physical significance and determination method of ξ potential. *Journal of Shandong Education Institute, 20(6),* 96–98. DOI 10.3969/j.issn.1008-2816.2005.06.033.
52. Taher, Z. J. (2017). *Effectiveness of polymer for mitigation of expansive soils (Master Thesis)*. Colorado State University, USA.